Available online at www.sciencedirect.com
ScienceDirect
Journal of Nuclear Materials 372 (2008) 358–366
journal of nuclear materials
www.elsevier.com/locate/jnucmat

Microstructure and leaching durability of glass composite wasteforms for spent clinoptilolite immobilisation

J.M. Juoi [a,*], M.I. Ojovan [a], W.E. Lee [b]

[a] Immobilisation Science Laboratory, University of Sheffield, Sir Robert Hadfield Building, Mappin Street, Sheffield S1 3JD, UK
[b] Department of Materials, Imperial College London, S Kensington Campus, London SW7 2AZ, UK

Received 6 November 2006; accepted 17 April 2007

Abstract

Simulated spent Cs-clinoptilolite waste was immobilised in a monolithic glass composite material (GCM) produced by a pressureless sintering at 750 °C for 2 h duration. The effects of waste loading from 1:1 up to 1:10 glass to waste volume ratio (37 up to 88 wt%) on the GCM wasteform microstructure and leaching properties were analysed. The open porosity ranged between 0.84 and ~13.2 % for the highest waste load. Significant changes occurred in the microstructure, phases present and wasteform durability at different waste loading. At waste loading up to 73 wt% of spent clinoptilolite, the GCM microstructure consists of several crystalline phases (clinoptilolite, sodalite, wollastonite and CsCl) that were fully encapsulated by a glass matrix. This leads to a low normalized leaching rate of Cs (remaining below 6.35×10^{-6} g/cm^2 day in a GCM with 73 wt% waste) during a leaching test for 7 days conducted using ASTM C1220-98. In GCM's with waste loading exceeding 73 wt%, the crystalline phases present (clinoptilolite and CsCl) were not fully encapsulated by the glass matrix hence the normalized leaching rate of Cs was as high as 9.06×10^{-4} g/cm^2 day at waste loading of $\geqslant 80$ wt%.

PACS: 81.05. Pj; 81.40.−Z; 61.10.−i

1. Introduction

Generally, GCM's are defined as materials that consist of both vitreous and crystalline phases. They can be classified somewhere between ostensibly fully amorphous vitreous wasteforms and ostensibly fully crystalline ceramic wasteforms and can be fabricated in several ways. These include the classic glass ceramic route [1] in which a fully melted system is crystallised on cooling or in a separate heat treatment operation or by deliberate dispersion of solid particles in a liquid (derived by melting or liquid phase sintering) which solidifies to a glass matrix. Several terminologies have been used in describing the end monolithic wasteform of a glass composite. Typical terms used are: glass bonded wasteform [2], ceramic wasteform [3], sintered glass [4], hot pressed glass matrix composite [5], reaction sintered glass [6], glass encapsulated wasteform [7], sintered aerogel [8], vitreous ceramic [9], glassy slag [10], glass ceramic [11] and glass-like material [12]. Much of these different terminologies have arisen from the different routes of producing the final glass composite or are related to the end features of the wasteform microstructure.

GCM's can be used with addition of glass compatible elements to immobilise glass-immiscible waste components such as sulphates, chlorides, molybdates and refractory materials requiring unacceptably high melting temperatures. Depending on the intended application, the major component of a GCM may be a crystalline phase with a vitreous phase acting as a bonding agent, or, alternatively, the vitreous phase may be the major component, with particles of a crystalline phase dispersed in the glass matrix. GCM's may be used to immobilise long-lived radionuclides (such as actinide species) by incorporating them into the

* Corresponding author. Fax: +44 114 2225943.
E-mail address: j.juoi@sheffield.ac.uk (J.M. Juoi).

0022-3115/$ - see front matter © 2007 Elsevier B.V. All rights reserved.
doi:10.1016/j.jnucmat.2007.04.047

more durable crystalline phases, whereas the short-lived radionuclides may be accommodated in the less durable vitreous phase. Historically, crystallisation of vitreous wasteforms has always been regarded as undesirable as it has the potential to alter the composition (and hence durability) of the remaining continuous glass phase which would (eventually) come into contact with water. However, there has been a recent trend towards higher crystallinity in ostensibly vitreous wasteforms so that they are more correctly termed GCM's [13]. This is particularly apparent in the development of hosts for more difficult wastes or where acceptable durability can be demonstrated even where significant quantities of crystals (arising from higher waste loadings) are present. Acceptable durability will result if the active species are locked into the crystal phases that are encapsulated in a durable glass matrix.

The purpose of this work is to analyse the microstructure and leach durability of a GCM designed to immobilise spent clinoptilolite arising from aqueous radioactive treatment facilities. Clinoptilolite is a natural zeolite which is used to remove radioactive contaminants such as ^{134,137}Cs from aqueous nuclear wastes arising from nuclear power plant operation, spent nuclear fuel reprocessing and various nuclear applications [14]. This is possible due to the ion-exchange capabilities, chemical and mechanical durability and availability of this inorganic mineral. Its crystal structure consists of $[SiO_4]$ and $[AlO_4]$ tetrahedra interconnecting with each other but with large channels enabling absorption of radionuclides.

To ensure safety during storage and disposal, spent waste sorbent needs to be immobilised in a solid wasteform to prevent escape of the mobile radionuclides into the surroundings. The current options for immobilisation matrices for spent ion exchangers are cementation, bituminisation, polymer encapsulation and vitrification. In some countries, high integrity containers are used for storage and/or disposal of spent ion exchange media, without incorporation into a solidification matrix. In addition, a one step treatment such as vitrification and incineration (used for organic ion exchangers only) is also an option. Each technology has benefits and drawbacks. Vitrification for example has a high waste loading and results in wasteforms with good durability. It has high volume reduction factor, (VRR) ~2–5 but requires high temperatures. Cementitious wasteforms have the lowest water durability at high waste loading. Additionally, cementation is characterised by an increase in volume e.g the VRR is <1. Also, cement based systems are characterised by high pH leading to desorption processes making them impractical for immobilisation of zeolites. Bituminisation products have good water durability but bitumen being organic is not fire safe.

In the current work, simulated spent clinoptilolite was immobilised in a monolithic GCM wasteform produced via a low pressure, low temperature sintering route. The GCM utilises the high durability of alkali borosilicate glass [15] to encapsulate the Cs-impregnated clinoptilolite (Cs-clino). With this approach, mobile radionuclides are retained by a multi-barrier system, comprising the crystalline form of the clinoptilolite and the borosilicate glass. To sinter the GCM, borosilicate glass was used with a composition close to nuclear waste glass applied in immobilisation of low level wastes in Russia [16] and in Hanford USA [17]. These glasses are characterised by good water durability and enable immobilisation of high-sodium content wastes. Thus in this approach, two waste streams, spent clinoptilolite and nuclear waste glasses, can be combined to produce a durable GCM which is acceptable for disposal. This study focused on the effect of waste loading on the GCM microstructure and durability.

2. Experimental

2.1. Materials

2.1.1. Cs impregnated clinoptilolite (Cs-clino)

Natural clinoptilolite obtained from the Mojave Desert, California via Nexia Solutions was used to produce the simulant waste. Ten grams of clino was exposed to an ion-exchange reaction with 1 M CsCl. After 72 h, the Cs impregnated clinoptilolite was extracted from solution and dried for 24 h at 110 °C. The concentration of Cs in Cs-clino, C_{Cs} was determined using an Agilent 4500 inductively coupled plasma mass spectroscopy (ICP-MS) instrument. The detection limit for Cs is 0.002 μg/L. XRD was carried out on Cs-clino powder using a Philips X-ray diffractometer 1130 over a scan range of 20–80° in 1°/min 2θ step sizes using Cu Kα radiation. Cs-clino particle size was determine using Coulter LS130 laser diffraction particle size analyser and its density was determined using the specific gravimetry method in water. Table 1 lists the results of Cs-clino characterisation.

C_{Cs} can be found based on clinoptilolite cation exchange capacity using Eq. (1).

$$C_{Cs} = \text{CEC} \times \text{A.M.U.}, \quad (1)$$

where CEC – cation exchange capacity, meq/g, A.M.U. – atomic mass units of Cs.

The CEC value of clinoptilolite ranges from 25 to 300 meq/100 g [18]. Thus the calculated value of C_{Cs} is in a range of 3.32–39.87 wt% and the 21 wt% of Cs determined by ICP-MS (Table 1) is in the range of cation exchange capacity of clinoptilolite.

Table 1
Cs-clino parameters

Analyses	Results
ICP-MS (wt%)	Cs – 21.0
XRD	Potassium sodium aluminium silicate hydrate $KNa_2Ca_2(Si_{29}Al_7)O_{72} \cdot 24H_2O$
Mean particle size (mm)	0.564
Density (g cm^{-3})	2.00 ± 0.23

Table 2
Properties of borosilicate glass used as matrix

Composition (wt%)	Oxide	Batch[a]	ICP[b]
	SiO_2	50.05	50.43
	Na_2O	16.72	14.00
	CaO	16.61	16.80
	Al_2O_3	2.60	2.74
	TiO_2	1.56	1.58
	B_2O_3	9.34	10.37
	Li_2O	3.12	2.46
	K_2O	–	0.75
	Total	100	99.13
T_g (°C)	488 ± 2		
Density (g cm^{-3})	2.60 ± 0.10		

[a] Calculated from batch composition.
[b] Calculated based on elemental composition obtain by ICP-AES.

2.1.2. Glass frit

The borosilicate glass used was produced from a glass batch melted at 1150 °C for 2 h in an alumina crucible. The cast glass was then annealed at 500 °C for 24 h. Glass was ground using an agate mortar and sieved to obtain glass powder with <75 μm particle size. The nominal glass composition was determined by inductively coupled plasma atomic emission spectroscopy (ICP-AES) and the glass transition temperature (T_g) was determined using differential thermal analysis (DTA) on a Perkin Elmer Pyris ITGA-DTA7 unit. Glass density was determined using the specific gravimetry method in water. Table 2 lists the properties of this glass.

Sintering has been carried out with both Cs-clino and borosilicate glass particles <75 μm in diameter with different waste loadings at 750 °C. The glass to Cs-clino volume ratios investigated were in the range of 1:1 to 1:10 (from 37 to 88 wt% waste loading). Mixtures of appropriate glass and Cs-clino powders were compacted at room temperature in a 13 mm diameter stainless steel die using 78.3 MPa uniaxial pressure. For comparison, samples were also made from compacted pellets of the host glass (borosilicate glass only) and from the simulated waste (Cs-clino only). Each compacted pellet was then sintered for 2 h at 750 °C with heating and cooling rates of 2 °C/min.

The mass fraction of waste in the GCM, F_{waste} is determined from the relationship

$$F_{waste} = \frac{m_{waste}}{m_{waste} + m_{glass}}, \tag{2}$$

where m_{waste} is the mass of Cs-clino and m_{glass} is the mass of glass.

The mass fraction of glass in the GCM sintered is defined as

$$F_{glass} = 1 - F_{waste}. \tag{3}$$

The mass fraction of Cs (f_{Cs}) in the unleached specimens was determined using Eq. (4).

$$f_{Cs} = F_{waste} \times C_{Cs}\left(\frac{1}{100\ \text{wt\%}}\right). \tag{4}$$

Table 3
Fraction of Cs, f_{Cs} in the unleached GCM wasteform

Glass to Cs-clino volume ratio	F_{glass}	F_{waste}	f_{Cs}
Glass only	1.00	0	0
1:1	0.63	0.37	0.078
1:2	0.41	0.59	0.123
1:3	0.31	0.69	0.144
1:4	0.27	0.73	0.153
1:5	0.20	0.80	0.169
1:10	0.12	0.88	0.185
Cs-clino only	0	1	0.21

The calculated values are given in Table 3.

GCM samples were cross sectioned, ground using SiC grinding wheel and polished using 6, 3 and 1 μm diamond paste. A JEOL JSM 6400 SEM operated in backscattered electron imaging (BEI) mode coupled with energy dispersive X-ray spectroscopy (EDS) analysis was used to determine the microstructure and identify the elements present as well as the distribution of Cs in the wasteform. XRD analysis of the glass powder, Cs-clino and each sintered GCM was carried out using a Philips X-ray diffractometer 1130 over a scan range of 20–80° in 1°/min 2θ step sizes using Cu Kα radiation. ICDD cards used to identify phases were clinoptilolite-Ca [39–1383], wollastonite [76–1846], sodalite [37–476], cesium aluminium silicate [41–569], cesium chloride [89–3627] and pollucite [29–407]. The porosity and density of the samples was determined using a Micromeritics mercury pore sizer model 9320.

Leaching tests were done in deionized water based on the ASTM C1220-98 standard at 40 °C for 7 days duration. The samples were contained in tightly closed teflon containers with specimen support made of teflon in it. The tests were run with a sample surface area to solution volume (S/V) ratio of 10 m^{-1} for each test. Here, the volume of leachant used was varied from 30 mL to 51 mL depending on the surface area of each sample used. The concentrations of dissolved Cs ion in the leachates (Table 4) were determined by inductively ICP-MS. The normalized leach rates (NR) were calculated using Eq. (5).

$$\text{NR}_{Cs} = \frac{A \cdot V}{(f_{Cs} \cdot \text{SA})t}, \tag{5}$$

where A – concentration of Cs in the leachate (g/L), V – volume of leachate (L), f_{Cs} – mass fraction of Cs in the

Table 4
Concentration of Cs in leachates, A after 7 days static test

Glass to Cs-clino volume ratio	A (g/L)
Glass only	Not detected
1:1	0.057×10^{-3}
1:2	0.025×10^{-3}
1:3	0.555×10^{-3}
1:4	0.799×10^{-3}
1:5	106.038×10^{-3}
1:10	439.995×10^{-3}
Cs-clino only	719.995×10^{-3}

unleached specimen, SA – specimen surface area, cm^2, t – duration of test, day.

3. Results

3.1. Characterisation of glass composite wasteform

The GCM wasteform microstructure produced with 1:1 glass to Cs-clino volume ratio sintered 2 h at 750 °C shown in Fig. 1(a) consists of a dark phase encapsulating grey angular (~11 μm long by 3 μm wide) crystals, and agglomerates of about 2.2 μm bright particles. In contrast, the microstructure of the Cs-clino sintered alone for 2 h at 750 °C in Fig. 1(b) comprises only loosely-packed bright grains. The microstructure of the sintered borosilicate glass (Fig. 1(c)) contains the same grey angular phase as seen in the GCM microstructure. EDS analysis of the bright particles present in GCM and sintered Cs-clino reveal it contains Na, Al, Si, K, Ca and Cs confirming these are clinoptilolite particles. The dark phase in the GCM consists of Na, Al, Si, Cl, K, Ca and Cs. These elements are the same as in the borosilicate glass composition used during the sintering except for Cs and Cl. This suggests that the borosilicate glass was a host glassy matrix encapsulating other crystalline phases and the Cs radionuclide present in the GCM. EDS spectra from the grey angular phase in the GCM and sintered borosilicate glass show that it contains only Ca and Si. Since no raw material with this composition was used at the processing stage, it can be deduced that the grey angular phase was due to the crystallisation of a calcium silicate phase from the host borosilicate glass.

XRD of GCM with 1:1 glass to Cs-clino volume ratio (Fig. 2(d)) suggests the presence of several crystalline phases after 2 h sintering at 750 °C. Phases identified based on matched positions and intensities of the GCM's XRD peaks with the ICDD database are clinoptilolite ($KNa_2Ca_2(Si_{29}Al_7)O_{72} \cdot 24H_2O$), wollastonite 2 M ($CaSiO_3$), sodalite ($Na_4Al_3Si_3O_{12}Cl$), cesium aluminium silicate ($CsAlSi_5O_{12}$) and cesium chloride (CsCl). Also traceable with a few weak XRD peaks is pollucite ($CsAlSi_2O_6$). The presence of clinoptilolite indicates that at least some of the Cs-clino remains in its original structure in the GCM. Clinoptilolite is a crystalline phase with monoclinic structure. The same phase was also identified when analysing the XRD peaks of Cs-clino sintered sample (Fig. 2(c)). Another identified phase, monoclinic wollastonite 2 M is likely to be the grey angular phase in the GCM microstructure (Fig. 1(a)) consistent with earlier

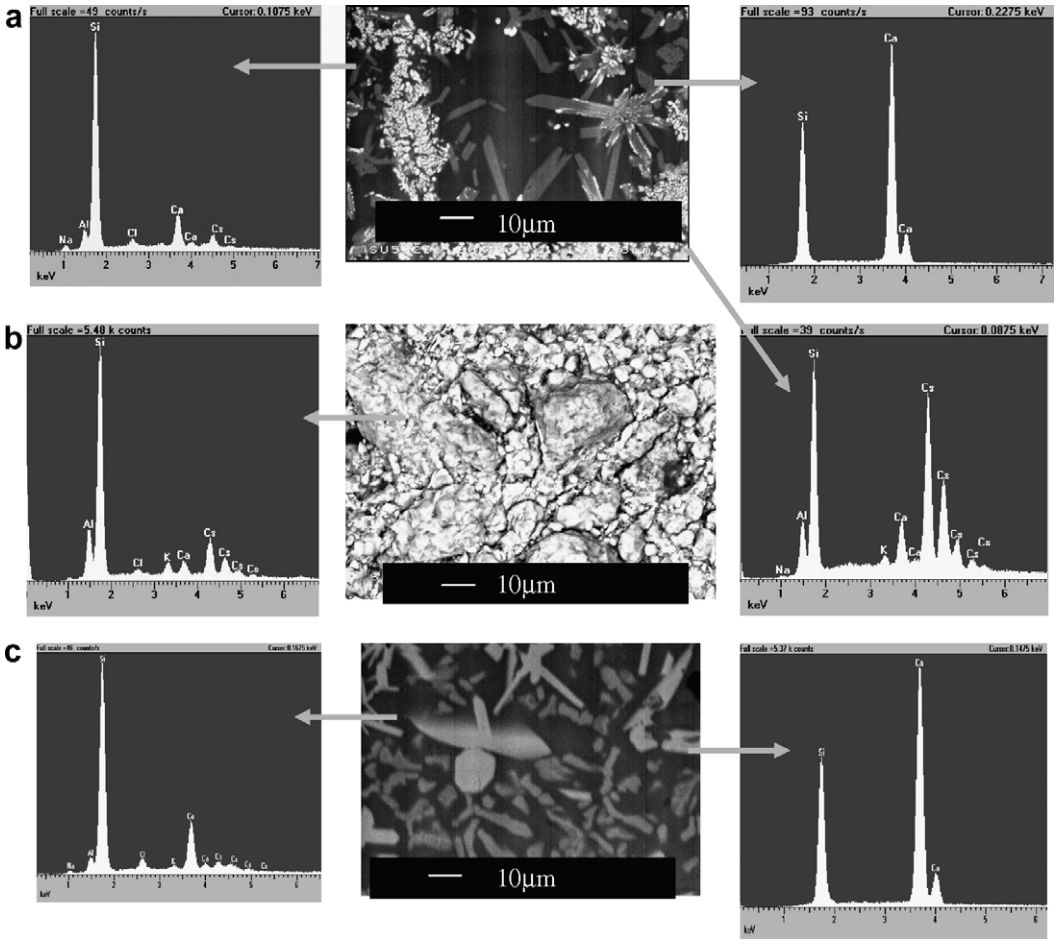

Fig. 1. BEI image and EDS of each phase of (a) GCM wasteform with 1:1 glass to Cs-clino volume ratio (b) sintered Cs-clino only and (c) sintered borosilicate only.

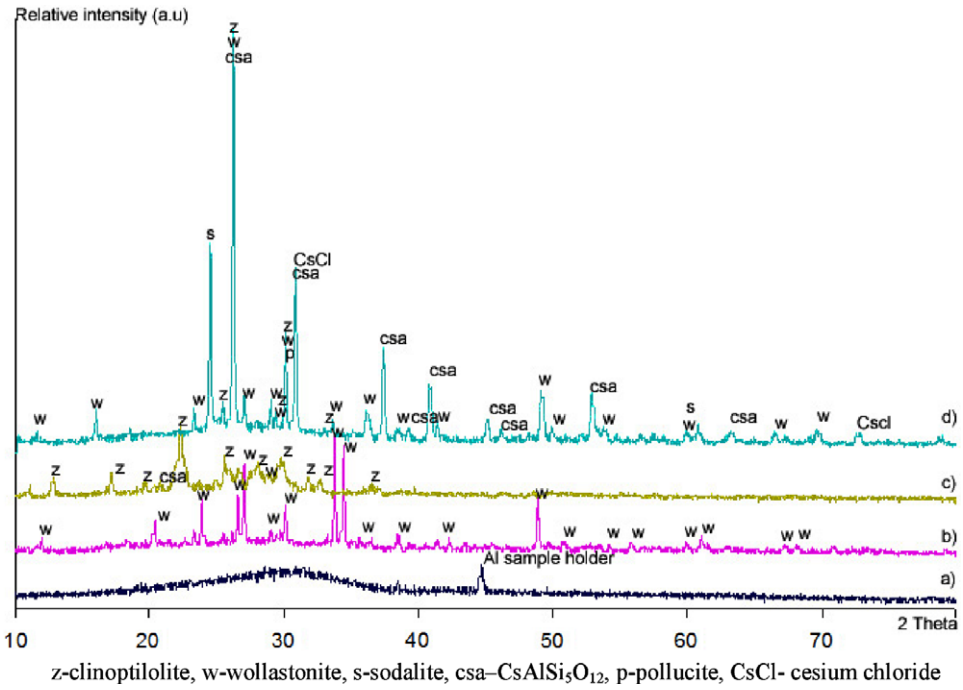

Fig. 2. XRD of (a) unheat-treated host glass, (b) sintered host glass only, (c) sintered Cs-clino only and d) sintered GCM wasteform with 1:1 glass to Cs-clino volume ratio after 2 h at 750 °C.

EDS analysis. Wollastonite was also identified in the sintered borosilicate glass (Fig. 2(b)). This confirmed that the wollastonite phase was due to crystallisation of the host borosilicate glass. Sodalite, $CsAlSi_5O_{12}$, pollucite and CsCl are crystalline phases that evolved during the GCM sintering. Presence of sodalite with a cubic structure was identified by several matched XRD peaks to the ICDD data with the highest intensity peak observed at $2\theta = 24.54°$. $CsAlSi_5O_{12}$ with orthorhombic structure is characterised with a series of XRD peaks positioned at higher 2θ (particularly at $2\theta = 45.17°$, 49.09° and 53.00°). This phase also identified in Cs-clino sintered alone sample (Fig. 2(c)). CsCl with cubic structure is detected with its XRD peaks observed at $2\theta = 30.85°$ and 72.79°. Apart from these three phases, pollucite with cubic structure was also traceable in the GCM wasteform with a few weak XRD peaks observed with some were overlapping with XRD peaks of phases discussed earlier. It should be noted that sodalite, $CsAlSi_5O_{12}$, CsCl and pollucite in the GCM wasteform are however not presence with distinguished features to be noticeable in its microstructure. Hence, it is not capable to discuss their existence in relation to the GCM microstructure observed earlier.

3.2. Effect of waste loading on microstructure

Analysis of GCM wasteform microstructures with increasing waste loading (Fig. 3) reveals that high waste samples did not densify well and larger pores could be observed. At the GCM waste loading exceeding 1:4 glass to Cs-clino volume ratio (73 wt% waste loading), the encapsulation of crystalline phase by the glassy matrix was poor and there was little glassy phase in the GCM produced. The glassy phase in this GCM appeared mainly at the edges of the crystalline particles and was locally concentrated in separate volumes rather than uniformly coating the crystalline particles. Elemental mapping showed that Cs was present in the crystalline phases as well as in the glass matrix although the concentration of Cs is much higher in the crystal.

3.3. Effect of waste loading on phase evolution

In the GCM sintered with 1:2 (Fig. 4(a)) and 1:4 (Fig. 4(b)) glass to Cs-clino volume ratio, the identified crystalline phases are clinoptilolite, wollastonite, sodalite, $CsAlSi_5O_{12}$ and CsCl. At this higher waste loading, agglomerates of bright particles were identified as sodalite. However, $CsAlSi_5O_{12}$ and CsCl are still not noticeable in the GCM microstructure. As the waste loading increases, the intensity of clinoptilolite peaks becomes more obvious. This was due to the increasing Cs-clino in the sintered samples. On the other hand, the wollastonite peak intensities decrease in the sintered GCM with higher waste loading as this was related to the reduced amount of glass used in the sintered GCM. Consequently, in GCM with 1:5 glass to Cs-clino volume ratio only clinoptilolite and $CsAlSi_5O_{12}$ were identified (Fig. 4(c)).

3.4. Effect of waste loading on density and porosity

Changes in bulk density and porosity were quantified as a function of waste loading. Fig. 5 indicates that as the waste loading increased, the bulk density of the GCM wasteform decreased due largely to the lower density of clinoptilolite compared to the host borosilicate glass

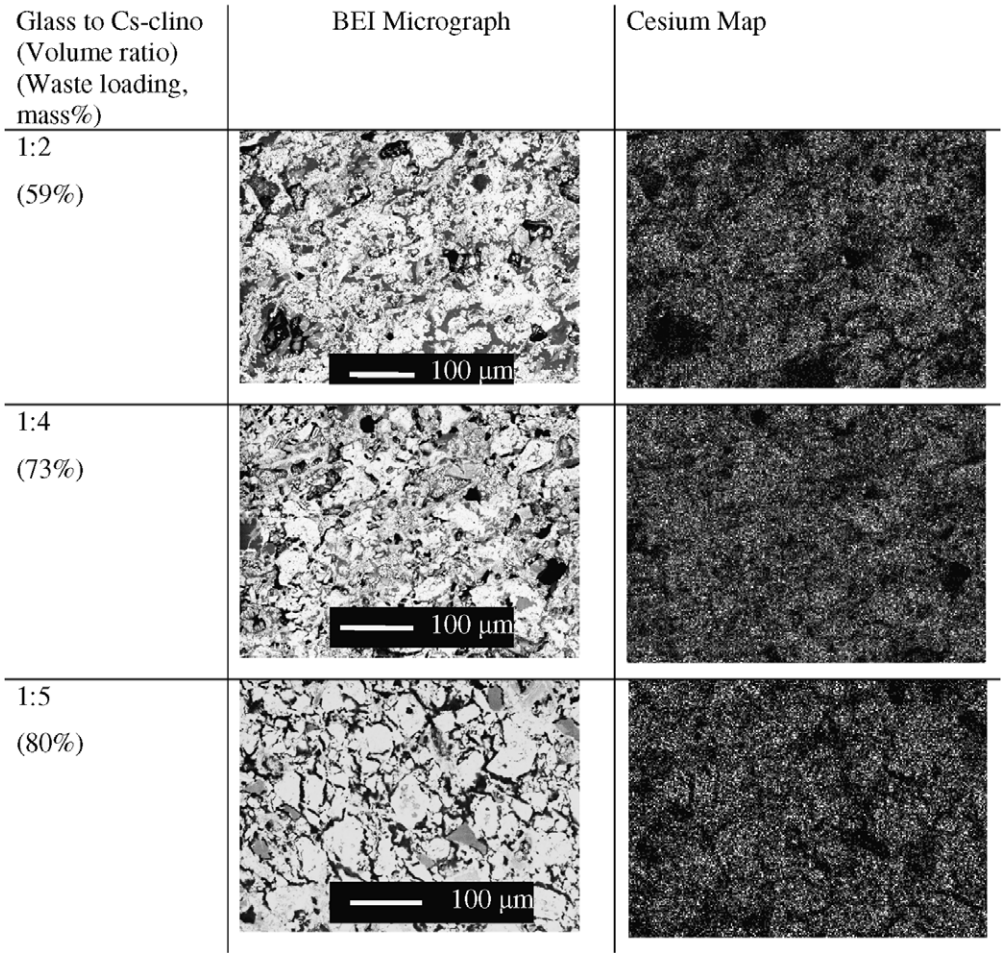

Fig. 3. Microstructural changes and Cs distribution in the GCM wasteform with increased waste loading.

(2.00 ± 0.23 compared to 2.60 ± 0.10 g cm^3). The decrease in GCM density at higher waste loading is also related to the increasing porosity observed.

3.5. Effect of waste loading on leaching durability

Leach testing results (Fig. 6) showed that normalized Cs leach rates increased gradually as the waste loading increased up to the 1:4 glass to Cs-clino volume ratio (73 wt% waste loading). However, it was also noticeable that the leaching rate at 1:2 glass to Cs-clino volume ratio was lower than that at lower (e.g. 1:1) glass to Cs-clino volume ratio. A drastic increase by more than 2 orders of magnitude of Cs leaching rate was observed for GCM at 1:5 glass to Cs-clino volume ratio (80 wt% waste loading). This can be explained by formation of percolating clusters made of inter-connected clino particles (Fig. 3). The normalized Cs leaching rates remain below 6.35×10^{-6} g/cm^2 day up to the waste loading of 73 wt%.

4. Discussion

GCM's made sintered with waste at volume ratios 1:1 to 1:10 glass to Cs-clino (37 up to 88 wt%) had a better leach resistance if they contained <1 vol.% porosity. This good durability was due to the macro- and micro-structure of the glass composite. In the GCM wasteform, the Cs radionuclides were retained in the clinoptilolite particles as well as the glassy matrix. In contrast, there was no glassy matrix to additionally encapsulate the Cs radionuclides in pure sintered Cs-clino. Microstructural studies showed good encapsulation of simulant waste sorbent in GCM at waste loading up to 73 wt%. The simulant sorbent was fully encapsulated by the glass matrix at this relatively high waste loading. Elemental analysis revealed that the simulant Cs radionuclide was partly retained in the clino as well as in the encapsulating glass matrix.

It was also found that apart from the clinoptilolite and glassy matrix, wollastonite ($CaSiO_3$), sodalite ($Na_4Al_3Si_3O_{12}Cl$), cesium aluminium silicate ($CsAlSi_5O_{12}$) and CsCl phases formed in the GCM produced. In addition, there is also a possibility of pollucite presence due to a few weak overlapping XRD peaks observed. Wollastonite evolved from the crystallisation of the host borosilicate glass during sintering, whereas the sodalite is the product of partial breakdown of Cs-clino and reaction of Na from the borosilicate glass with Cl from Cs-clino. It should be worth mentioning that the presence of Cl in the simulated

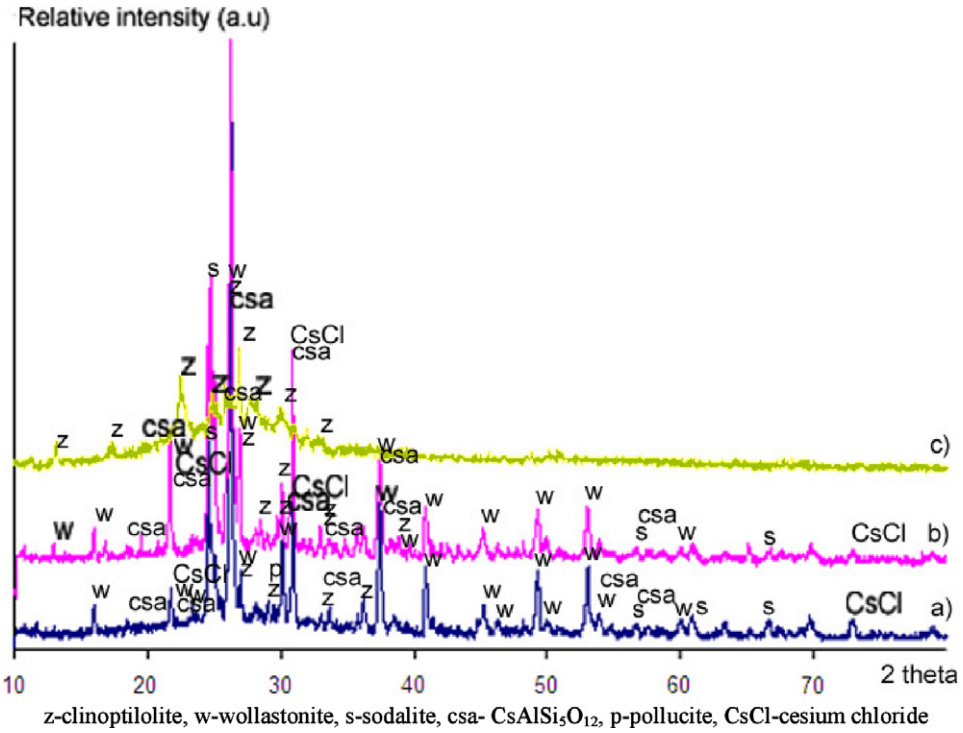

Fig. 4. XRD of GCM with glass to Cs-clino volume ratio respectively (a) 1:2, (b) 1:4 and (c) 1:5 after 2 h at 750 °C.

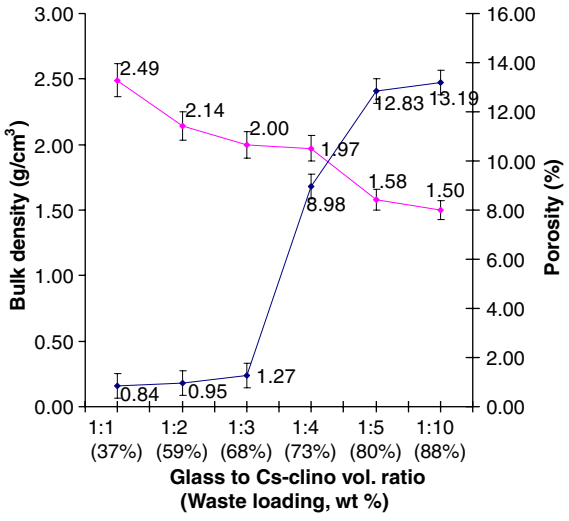

Fig. 5. Bulk density and porosity of glass composite wasteform with the increase of waste loading.

Cs-clino is to be expected either in a form of free CsCl or occluded into the clinoptilolite structure. This is due to no washing step was carried out after the impregnation of Cs into the clinoptilolite using 1 M CsCl solution. In such a way the simulated waste could be considered bearing the common free salt that possibly presence in radioactive waste treatment environment for instance, CsCl is a typical formed of waste bearing radioactive ^{137}Cs at the Hanford Site [19]. The remaining Cl from the Cs-clino is also likely to led the presence of CsCl in the GCM. In the other hand, $CsAlSi_5O_{12}$ is a phase that evolved possibly due to the effect of heating to the Cs-loaded clinoptilolite. This could be deduced as this phase also identified in Cs-clino sintered alone (without addition of glass). This phase also has been reported to form on heating certain Cs-loaded modernite, another type of zeolite [20].

The relatively high percentage of crystallinity in the sintered borosilicate glass used, as well as from the effect of heating Cs-clino with glass particles during sintering, contributes towards the overall high crystallinity of the sintered GCM. Analysis of microstructures with increasing waste loading showed that at lower waste loading (e.g 1:1), wollastonite appeared as ~11 μm long by 3 μm wide grey angular crystal. As waste loading increases, this phase is present with a shorter (~6 μm) grey rounded morphology (e.g 1:2) throughout the wasteform. Consequently the GCM with 1:2 glass to Cs-clino waste loading had a lower leaching rate. Based on this analysis, it is suggested that the angular wollastonite–matrix interfaces introduce additional pathways for Cs diffusion and leaching in water.

At present, the effect of sodalite, $CsAlSi_5O_{12}$ and CsCl in the GCM could not be discussed directly in relation to the GCM leaching performance. This is due to current work carried out could not serve the purpose of comparing the effect of various phases present. However, the presence of sodalite and $CsAlSi_5O_{12}$ could generally contribute towards improving GCM durability. Sodalite with chlorine as parts of its cubic crystal structure is one of a few natural mineral that contains insoluble chloride. Because of its potential in retaining chloride, sodalite was examined as a possible mineral wasteform for the waste from the electrofining of spent nuclear fuel [21]. Meanwhile, $CsAlSi_5O_{12}$

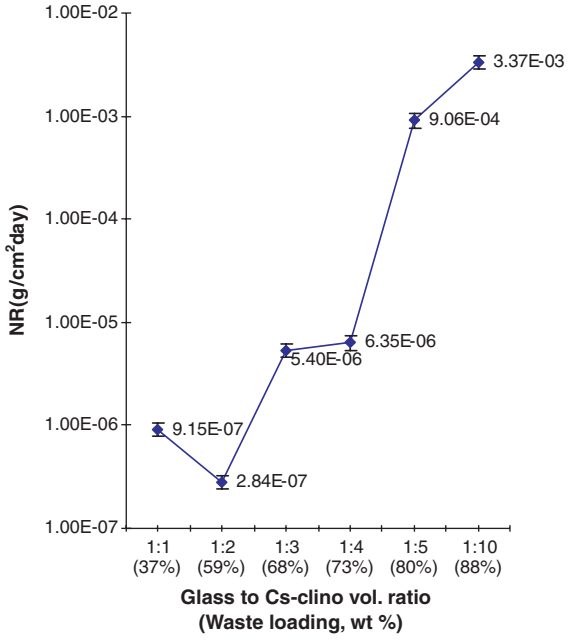

Fig. 6. Cesium normalized leaching rates of glass composite wasteform with the increase in waste loading.

has been reported with a good leach-resistant property so as to be studied as a potential host for ^{137}Cs immobilisation [22]. However, the presence of CsCl in the GCM is considered to be undesirable component, as this free salt phase could lead to poor chemical durability. Consequently, the efforts on eliminating this free salt phase will be essential in further development of the GCM wasteform. This could be done via optimisation of sintering parameters.

At higher waste loading, clinoptilolite and $CsAlSi_5O_{12}$ are the major phases in the GCM with lower wollastonite and glassy phase. This is due to the low fraction of glass used at higher waste loading. It was also found that GCMs with higher waste loading have lower density and higher porosity observed. Consequently, the leaching rate increased with increased waste loading. The increase of porosity can be associated with less glass matrix available. Moreover, clinoptilolite being naturally porous is expectedly to contribute towards the higher porosity of GCM with higher Cs-clino loading. Higher porosity of GCMs at higher waste loadings cannot be attributed to possible release of free chlorine as CsCl has the boiling point at 1290 °C. Moreover, no gas bubbles were found in the glassy phase of GCM.

From an economical and repository space utilisation perspective it is desired to have the highest waste loading in the developed GCM wasteform. However, the waste loading increase is limited by the need for an acceptable (low) leaching rate. In our work, the normalized leaching rates of Cs remains below 6.35×10^{-6} g/cm^2 day with up to 73 wt% waste loading. NR_{Cs} were significantly lower compared to Portland and alumina cement with 12–19 mass% spent ion exchange resin [23] and cement-bentonite clay wasteforms with waste loads of 290–350 kg/m^3 [24] which has a leaching rate of Cs in a range of $\sim 10^{-3}$–10^{-4} g/cm^2 day. The Cs normalized leaching rate becomes $>9.06 \times 10^{-4}$ g/cm^2 day for GCMs containing $\geqslant 80$ wt% of spent clinoptilolite. This drastic increase can be explained by formation of percolating clusters made of inter-connected clino particles (see Fig. 3). According to percolation theory the leaching rate has an universal behaviour near the threshold of formation of percolating clusters [25,26].

$$NR_{Cs} = \frac{NR_{Cs}(0)}{(f_{Cs} - f_{Thr})^{\beta}}, \quad (6)$$

where $NR_{Cs}(0)$ is the normalized leaching rate far from the percolation threshold which we assessed as $f_{Thr} \sim 0.8$ (C_{Cs}/100 wt%) and $\beta = 0.41$ is the universal critical exponent [27]. The increase of NR_{Cs} at $f > f_{Thr}$ was also related to higher porosity at higher waste loadings (Fig. 5).

5. Conclusion

Microstructural characterisation shows good encapsulation of simulant waste sorbent in a GCM at waste loading up to 73 wt%. The normalized leaching rate of Cs remains below 6.35×10^{-6} g/cm^2 day with up to 73 wt% waste loading. The normalized leaching rate of Cs becomes as high as 9.06×10^{-4} g/cm^2 day for GCM containing $\geqslant 80$ mass% of spent clinoptilolite. Waste loading must, therefore be limited to $\sim$73 wt% for spent clinoptilolite immobilisation in this particular GCM. Further work should take into consideration eliminating presence of free salt via optimisation of sintering parameter.

References

[1] W.E. Lee, M.I. Ojovan, M.C. Stennett, N.C. Hyatt, Adv. Appl. Ceram. 105 (1) (2006).
[2] M.A. Lewis, D.F. Fischer, Ceram. Trans. (Environmental and waste management issues in ceramic and nuclear industries) 45 (1994) 277.
[3] M.A. Lewis, M. Hash, D. Glandorf, Mater. Res. Soc. Symp. Proc. 465 (1997) 433.
[4] A.M. Bevilacqua, N.B.M.D. Bernasconi, D.O. Russo, M.A. Audero, M.E. Sterba, A.D. Heredia, J. Nucl. Mater. 229 (1996) 187.
[5] A.R. Boccacccini, S. Atiq, R.W. Grimes, Adv. Eng. Mater. 5 (7) (2003) 501.
[6] W.L. Gong, W. Lutze, R.C. Ewing, J. Nucl. Mater. 278 (2000) 73.
[7] I.W. Donald, B.L. Metcalfe, R.S. Greedharee, Mater. Res. Soc. Symp. Proc. 713 (2002) JJ2.1.1.
[8] T. Woigner, J. Reynes, J. Phalippou, J.L. Dussossoy, N. Jacquet-Francillon, J. Non-Cryst. Solids 225 (1998) 353.
[9] X. Feng, W.K. Hahn, M. Gong, W. Gong, L. Wang, Ceram. Trans. (Environmental Issues and waste management technologies in the ceramic and nuclear industries) 72 (1996) 123.
[10] I. Roth, T. Metzger, Ceram. Trans. (Environmental Issues and waste management technologies) 61 (1995) 365.
[11] R.S. Baker, J.R. Berreth, Ceram. Trans. (Nuclear Waste Management III) 13–22 (1990) 9.
[12] M.I. Ojovan, W.E. Lee, Glass Technol. 44 (6) (2003) 218.
[13] J.M. Juoi, M.I Ojovan, W.E. Lee, in: Proceedings of ICEM'05, September 4–8, Glasgow, Scotland, ICEM05-1069, ASME, 2005.
[14] A. Dyer, D. Keir, Zeolites 4 (July) (1984) 215.
[15] M.I. Ojovan, W.E. Lee, An Introduction to Nuclear Waste Immobilisation, Elsevier, Amsterdam, 2005.

[16] B.P. McGrail, D.H. Bacon, J.P. Icenhover, F.M. Mann, R.J. Puigh, H.T. Schaef, S.V. Mattigod, J. Nucl. Mater. 298 (2001) 95.
[17] M.I. Ojovan, S.A. Dimitriev, F.A. Livanov, A.P. Kobelev, S.V. Stefanovsky, Glass Technol. 46 (1) (2005) 28.
[18] A.E. Osmanlioglu, J. Hazard. Mater. 137 (1) (2006) 332.
[19] M.G. Mesko, D.E. Day, B.C. Bunker, Waste Manage. 20 (2000) 271.
[20] S. Forberg, T. Westermark, L. Falth, Sci. Bas. Nucl. Waste Manage. 3 (1981) 227.
[21] C. Pereira, Ceram. Trans. 61 (1995) 389.
[22] T. Adl, E.R. Vance, J. Mater. Sci. 17 (1982) 849.
[23] I. Plecas, R. Pavlovic, S. Pavlovic, J. Nucl. Mater. 327 (2004) 171.
[24] V.N. Epimakhov, M.S. Oleinik, Atom. Energy 99 (2005) 607.
[25] I.V. Golubtsov, M.B. Kachalov, M.I. Ozhovan, Chemistry 31 (1992) 470.
[26] A.S. Barinov, I.A. Sobolev, M.I. Ozhovan, Atom. Energy 65 (1998) 977.
[27] M. Sahimi, Application of Percolation Theory, Taylor & Francis Publisher, London, 1994.